The surprising rolling spool: Experiments and theory from mechanics to phase transitions

Article *in* European Journal of Physics · July 2014

DOI: 10.1088/0143-0807/35/5/055011

The surprising rolling spool: experiments and theory from mechanics to phase transitions

P. Onorato [a] , M. Malgieri [a] , P. Mascheretti [a] and A. DeAmbrosis [a]

[a] Department of Physics University of Pavia, Via Bassi 6, I-27100 Pavia, Italy
pasquale.onorato@unipv.it massimiliano.malgieri01@ateneopv.it anna.deambrosisvigna@unipv.it

An asymmetric rolling spool can be investigated as a simple model for a second-order phase transition. At low energy it undergoes librational motion around the equilibrium position while at high energies its motion becomes rototransational. The analysis of its dynamics shows that when approaching the critical energy, the period of oscillation diverges and this suggests the transition from one phase to the other.
We thus show that the concept of 'phase transition', useful to describe the behaviour of a variety of thermodynamic systems, can be actualized in this simple mechanical system.
Moreover, a tight analogy can be found between the rolling spool's behaviour and the Tomlinson model of sliding friction. This analogy allows to interpret the critical switch of static friction near the threshold of motion as a phase transition. The rolling spool can be easily constructed and used as an hands-on type experiment. Quantitative measurements of its motion were carried out through an open source Video Analysis software.

I INTRODUCTION

In recent years several works have highlighted analogies between simple mechanical models and phase transitions in thermodynamic systems [1-7] starting from the assumption that one-dimensional mechanical systems can represent models of thermodynamic behaviour [8-12].
In this work we analyze, both experimentally and theoretically, a mechanical system that can be used to demonstrate the underlying mechanism of phase transitions. It consists of a rolling spool with an extra mass, which has the purpose of breaking the symmetry of the system. The device is analogous to the so-called unbalanced disk rolling on a plane described in refs. [13-15] Here we focus on the comparison between experimental results an theoretical predictions and we show how the rolling spool can represent a simple model for second-order phase transitions.
During the motion of the rolling spool, the friction force changes direction producing the leftward or rightward acceleration of the system. Observing and analyzing the motion can help students to refute right from the start the idea that friction always has a resistive effect, generating a force that invariably opposes motion. Moreover a careful quantitative discussion will show that the normal force producing friction is not equal to the weight and depends on the motion of the spool. Actually we originally designed the spool with the aim of highlighting the role of friction in rolling motion[16], but it has also proven useful for investigating various different topics in physics such as anharmonic oscillations [17-20] and phase transitions.
Due to an extra mass displaced from the geometric centre of the circle, the asymmetric rolling spool displays two different kinds of motion: oscillatory (librational) at low energies and roto-translational (rolling) at high energies. The period of the oscillations depends on the amplitude (so it is anharmonic) and diverges when the amplitude approaches a critical value i.e. when the motion switches from librational to rotational. We show that this divergence can be associated with a critical phenomenon and that the complex concept of phase transition that is used to describe thermodynamic systems (for example the transition of a monoatomic gas to solid) can be also applied to this simple mechanical system. [1-7] In fact, according ref.[7], when qualitatively different orbits appear in a mechanical system for different values of energy, these orbits may be intuitively labelled as distinct thermodynamic phases. Therefore, by considering the possible configurations of this simple mechanical system we can gain insight into the meaning of phase transition for more complex thermodynamic systems.
The theoretical apparatus needed to study the phase transition for the rolling spool also applies to the explanation of the critical switch of static friction near the threshold of motion in terms of phase transition. In fact a tight analogy exists between the rolling spool's behaviour and the Tomlinson model of sliding fiction [21], suggested by Prandtl in 1928 [22] and used as the basis for many investigations of frictional mechanisms on the atomic scale [23]. Starting from this formal analogy it is possible facilitate students' understanding of friction at a microscopic scale.
Our approach for studying the above concepts and analogies is based on the combination and comparison of experimental, theoretical and numerical analyses. Experiments are assisted by the open source Tracker Video analysis tool [24-25]

II EXPERIMENTAL RESULTS

The rolling spool is made with two CDs glued to a small wooden cylinder; an extra mass, M_W is fastened to one of the CDs in a non-central position. The precise geometrical parameters of the spool are specified in Fig. 1.
All measurements were carried out by acquiring videos of the motion of the spool through a 30 fps video camera, and then analysing the videos using the Tracker software. [24] We recorded videos of the spool rolling on a horizontal plane and performing free oscillations.

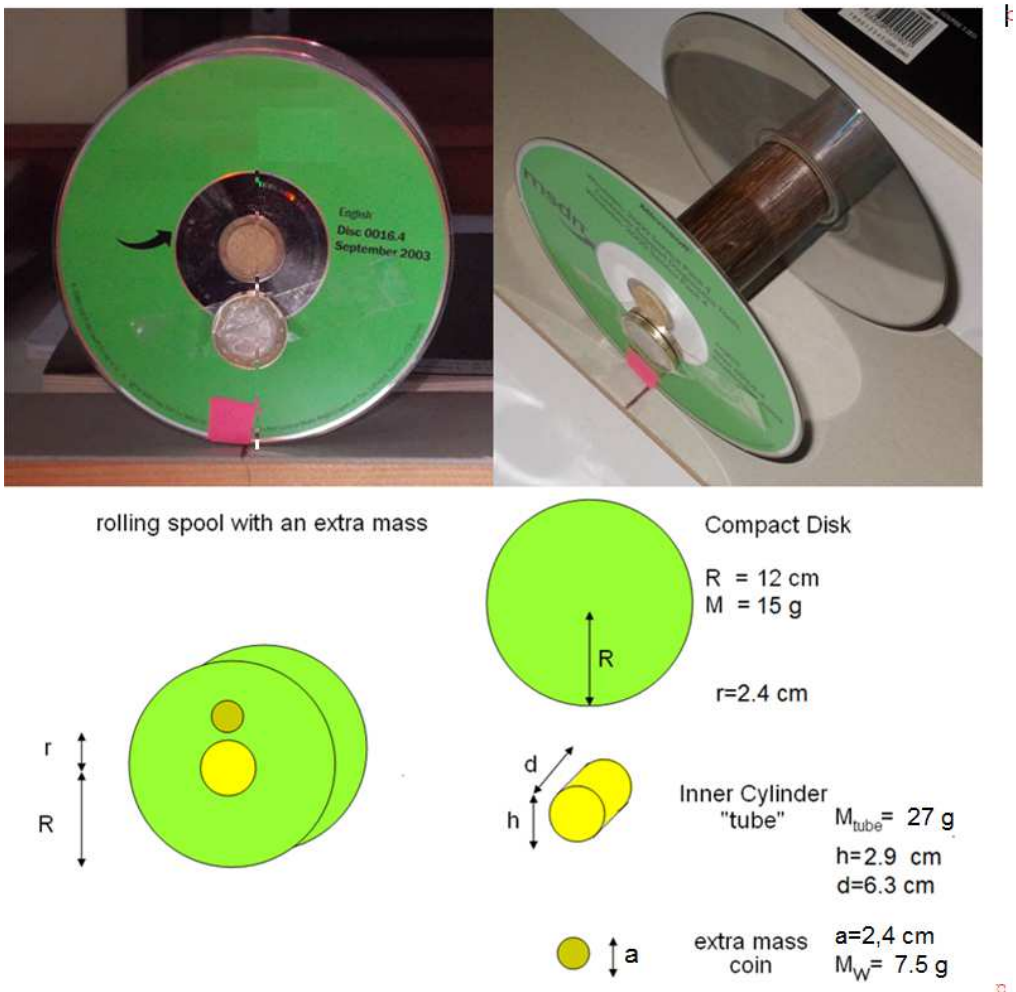

Figure 1 The rolling spool (made with two CDs) with an extra mass (a coin) breaking the symmetry of the system; schematic representation of the spool displaying the values of its geometrical parameters.

Rolling condition We preliminary checked the condition of rolling without slipping for the spool. Measurements reported in Fig.2.A confirm the proportionality between the velocity of the geometrical centre of the spool and its angular velocity, with a slope $m \approx 0.061 \pm 0.003\, m$, in agreement with the measured value of the CD radius $R \approx 0.060 \pm 0.001 m$.

Rolling on the horizontal plane In Fig.2.B the acceleration of the geometrical centre is represented as a function of the linear displacement x from the equilibrium position x_0 showing a strongly non linear behaviour, fitted by a curve $a_c = A \sin(\frac{x_c}{R_E} + \delta\vartheta) + B$ (see the theoretical analysis in the next

section). The experimental values of the parameters, obtained by fitting the data with Tracker, are $A = 0.35 \pm 0.01 \, m/s^2$, $R_E = 0.059 \pm 0.002 \, m$, $\delta\vartheta = 0.1 \pm 0.1 rad$ and $B = 0.005 \pm 0.01 \, m/s^2$.

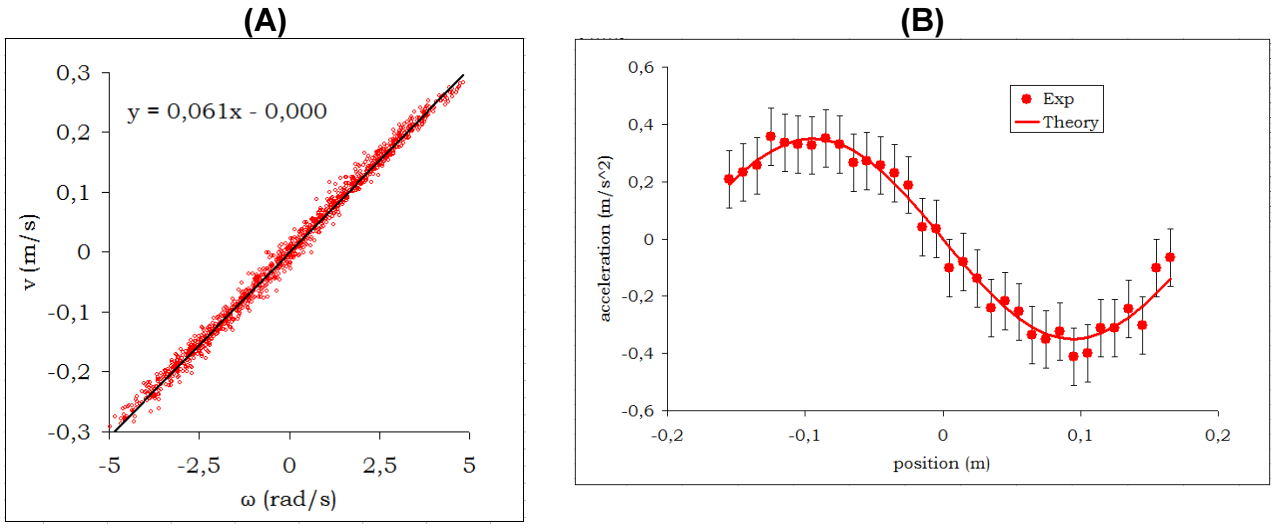

Figure 2 (A) Measurements and fitting straight line showing the proportionality between the velocity of the geometrical centre of the spool and its angular velocity (B) Measurements and fitting curves for the acceleration of the geometrical centre of the spool

In Fig.3 the measured period of oscillation as a function of the amplitude is represented. Data show a constant period ($\tau \approx 2.5 \pm 0.1 s$) for small amplitude oscillations and a divergence of the period value as the amplitude approaches π. A theoretical interpretation of these results will be discussed in the following section.

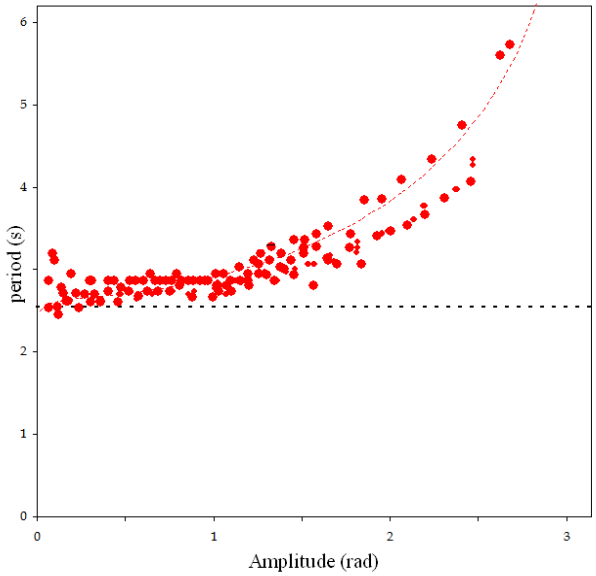

Figure 3 Experimental results for the measured period τ as a function of the amplitude of oscillation. Circles correspond to the experimental results while the dashed line corresponds to the theoretical result.

Figure 4 shows the dependence of the velocity v of the geometrical centre on the position x (phase space). The graph displays the characteristic eye-shaped contour associated with anharmonic oscillations for large amplitudes, as opposed to the elliptical shape of the phase space contour of the harmonic oscillations for small angles. Open orbits, corresponding to rotational motion of the spool are also shown. The separatix is the curve corresponding to the energy necessary for the spool to make a full circle (an oscillation of amplitude π). It separates (hence the name) the phase space into two distinct areas. The region inside the separatrix includes all those phase space curves which correspond to oscillating motion back and forth of the rolling spool, whereas the region outside the separatrix contains all the phase space curves which correspond to the motion with the spool continuously rolling on the plane.

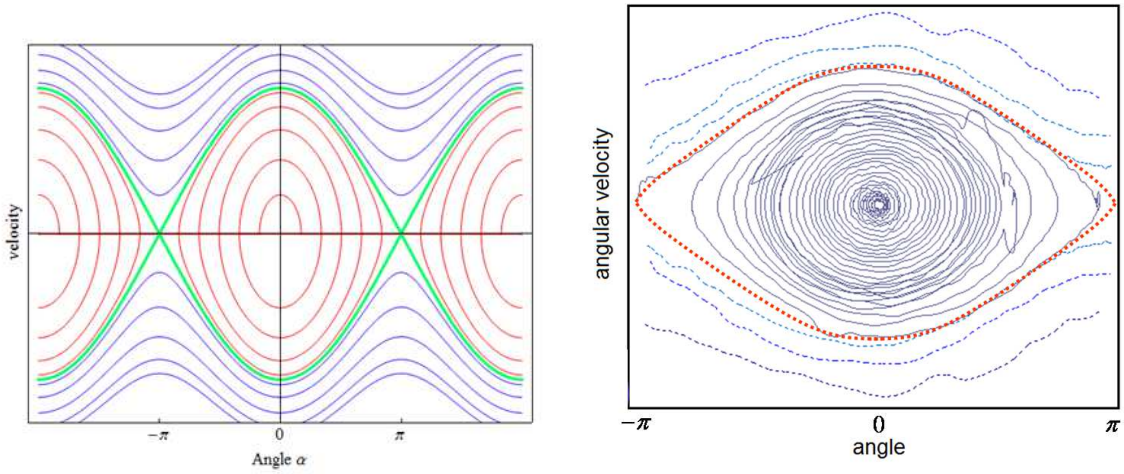

Figure 4 (A) Phase portraits for the rolling spool. The green line is a separatrix referring to the boundary between the librational closed orbit and rotational open orbits. (B) Experimental "phase space". The dependence of the velocity *v* on *x* with a characteristic eye-shaped contour associated with the nonlinear asymmetric nature of the force. In comparison, the phase space of a harmonic oscillator is elliptical. The small effect of the dissipative forces results in an inward clockwise spiral trajectory.

III THEORETICAL DESCRIPTION

Kinetic energy

In order to describe the dynamical behaviour of the system, we first write the general form of the kinetic energy in the laboratory frame, in the hypothesis that the spool rolls without slipping. We will show that this condition is satisfied by our system.

$$K(\vartheta,\dot{\vartheta}) = \frac{1}{2}\left[I_{core} + I_{M_W} + M_{core}R^2 + M_W\left(R^2 + r^2 - 2Rr\cos\vartheta\right)\right]\dot{\vartheta}^2 = \frac{I_{eff}(\vartheta)}{2}\dot{\vartheta}^2 \qquad (1)$$

where $M_{core} = M_{CD} + M_{tube}$ in the notations of Fig. 1. In the figure the values of all parameters of the system are reported. We can choose as only Lagrangian variable the angle θ between the radius passing through the extra mass position and the vertical axis The centre of mass is located at distance $d_{CM} = r_W M_W / M_W + M_{core}$ from the centre of the cylinder. From Eq. (1) an effective, angle-dependent moment of inertia can be identified for the spool as:

$$I_{Eff}(\vartheta) = I_{core} + I_{M_W} + M_{core}R^2 + M_W\left(R^2 + r^2 - 2Rr\cos\vartheta\right) = I_0 - 2M_W Rr\cos\vartheta = I_0\left(1 - \lambda\cos\vartheta\right) \quad (2)$$

where we have introduced the parameter $\lambda = \frac{2M_W rR}{I_0}$. The value of λ provides a measure of the asymmetry of the system. Note that $I_{Eff}(\vartheta)$ corresponds to $I_P(\vartheta)$ as calculated by ref.[27] and [28].

Potential energy

The forces acting on the rolling spool are gravity, normal force and static friction. We can take the equilibrium position, x_{eq} as the origin of the horizontal position axis, and make it correspond to $\vartheta = 0$ so that, when the spool rolls without slipping, the position and velocity of the geometrical centre of the disk are $x = R\vartheta$ and $v_C = R\dot{\vartheta}$ respectively. The gravitation potential energy of the system is given by

$$U(\vartheta) = M_W gr(1 - \cos\vartheta) \qquad (3)$$

Combining equations (2) and (3), with the conservation of energy, $E = K + U$, one obtains

$$\dot{\vartheta}(\vartheta)^2 = 2\frac{\left(E - U(\vartheta)\right)}{I_{eff}(\vartheta)} = 2\frac{M_W gr\left[\cos(\vartheta) - \cos(\vartheta_i)\right]}{I_0(1 - \lambda\cos(\vartheta))} \tag{4}$$

Where the second expression is valid if, as in our case, the spool is initially at rest.
To find the equation of motion we multiply Eq. (4) by $I_{EFF}(\vartheta)$; we derive both sides with respect to time, and divide the result by the angular velocity $\dot{\vartheta}$ [28] to obtain[1]

$$\ddot{\vartheta} = -\frac{\left[g + R\dot{\vartheta}^2\right]}{I_0\left(1 - \lambda\cos\vartheta\right)} M_W r\sin(\vartheta)$$

and $a_c = R\ddot{\vartheta}$.
For our spool the condition of small λ is verified (in our case $\lambda \approx 0.075 \pm 0.05$), then

$$a_c = R\ddot{\vartheta} \approx \frac{\lambda}{2} g\sin(\vartheta) = \frac{\lambda}{2} g\sin(\frac{x_c}{R}),$$

By comparing this result with the experimental values for a_c in Fig.2.B we find a very good agreement. In particular, the measured amplitude $A = 0.35 \pm 0.01\, m/s^2$ fits well with the theoretical value $\frac{\lambda}{2} g \approx 0.37 \pm 0.02\, m/s^2$.

By using the equation of motion it is possible verify that our spool rolls without slipping on a horizontal plane. We can start from the forces acting on the rolling spool, represented in Fig.5. The frictional force, $F_f = M_{tot} a^x{}_{cm}$, induces the horizontal acceleration of the centre of mass while the normal and the gravitational forces produce the vertical acceleration of the centre of mass, $F_N - M_{tot} g = M_{tot} a^y{}_{cm}$.

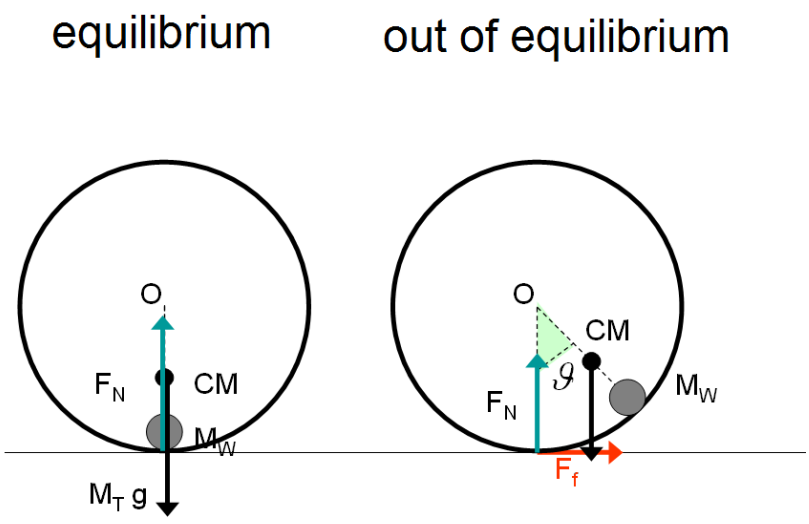

Figure 5. Forces on the rolling spool: gravity on the centre of mass, normal force, and friction force, the only one acting along the horizontal plane.

The condition on friction force $|F_f| \le \mu_s F_N$ implies that the rolling spool rolls without slipping if

[1] Using a different but equivalent approach, one could write from the start the Lagrangian $L(\vartheta, \dot{\vartheta}) = K(\vartheta, \dot{\vartheta}) - U(\vartheta)$ and obtain again the full equation of motion $\ddot{\vartheta} I_{Eff}(\vartheta) = -M_W r\sin\vartheta\left(g + R\dot{\vartheta}^2\right)$

$$\mu_s \geq \frac{a^x{}_{cm}}{g + a^y{}_{cm}} = \left| \frac{R\ddot{\vartheta} - d_{CM}\left(\ddot{\vartheta}\cos\vartheta + \dot{\vartheta}^2 \sin\vartheta\right)}{g + d_{CM}\left(\ddot{\vartheta}\sin\vartheta + \dot{\vartheta}^2\cos\vartheta\right)} \right|$$

The value of the right term can be evaluated from the constructive parameters of the rolling spool starting from $\ddot{\vartheta}_{MAX} = \frac{M_W r\left(g + R\dot{\vartheta}^2_{MAX}\right)}{I_0\left(1-\lambda\right)}$ (from the equation of motion) and $\dot{\vartheta}^2_{MAX} = \frac{4M_W gr}{I_0\left(1-\lambda\right)}$ (from eq. 4) . By writing $\mu_S \geq \left| \frac{R\ddot{\vartheta}_{MAX} + d_{CM}\left(\ddot{\vartheta}_{MAX} + \dot{\vartheta}^2_{MAX}\right)}{g - d_{CM}\left(\ddot{\vartheta}_{MAX} + \dot{\vartheta}^2_{MAX}\right)} \right|$ We obtain $\mu_s \geq 0.060$ [2]. Since the coefficient of static friction for wooden planes with plastic materials is above 0.2 we can surely confirm that the condition of rolling without slipping is satisfied. This is confirmed by the experimental result represented in Fig.2.A that shows proportionality between the velocity of the geometrical centre and the angular velocity of the spool.

Oscillation period

We can now find the period of the oscillations of the rolling spool. Since the acceleration of the geometrical centre of the spool $a_x = \ddot{\vartheta}R$ is not linearly dependent on the displacement from equilibrium position the oscillation period τ strongly depends on the amplitude, ϑ_0 , of the oscillations and can be expressed as

$$\tau(\vartheta_0) = \oint \frac{d\vartheta}{\dot{\vartheta}(\vartheta)}$$

where the integral is along the closed orbit and $\dot{\vartheta}(\vartheta)$ is given by eq.(4) with. In Fig.3 the experimental results for the measured period τ as a function of the amplitude of oscillation (circles) are compared with the theoretical result obtained by a numerical integration (dashed line). A good agreement between predicted and measured values is found. The graph of τ vs θ shows the typical features of anharmonic motion.

Moreover, the function $\dot{\vartheta}(\vartheta)$ *(angular velocity versus angle)* shows a characteristic not elliptic contour (e.g. eye-shaped). The experimental data on the dependence of the velocity of the centre of the spool on the angle, reported in Fig.4.B, are in good agreement with the theoretical predictions displayed in Fig.4.A.

In the limit of small oscillations amplitude we can assume that

$$\ddot{\vartheta} = -\frac{\left[g + R\dot{\vartheta}^2\right]}{I_0\left(1 - \lambda\cos\vartheta\right)} M_W r \sin(\vartheta) \approx -\frac{gM_W r}{I_0\left(1-\lambda\right)}\vartheta$$

i.e. the (angular) frequency is

$$\omega = \frac{2\pi}{\tau_0} = \sqrt{\frac{M_W rg}{I_0(1-\lambda)}} \qquad (5)$$

Thus for small amplitude (harmonic) oscillations the spool is analogous to a simple pendulum with an effective length (radius of gyration [29]) $\ell_{eff} = I_0\left(1-\lambda\right) \Big/ M_W r$

[2] It can be shown that, for small values of the parameter λ , the lower bound estimate for the friction coefficient can be expressed as a function of λ only. Through a power series expansion one finds $\mu_S \geq \frac{\lambda}{2}\left(1 + \frac{27}{4}\lambda + o\left(\lambda^2\right)\right)$.

Using eq.(5) we find a theoretical value of $\tau = 2.45 \pm 0.15 s$ in good agreement with the measured period for small amplitude oscillations $\tau = 2.5 \pm 0.1 s$.

IV. PHASE TRANSITION

When the amplitude approaches a critical value, the period of oscillation of the rolling spool diverges. We argue that such divergence signals the presence of a phase transition corresponding to the appearance of two distinct phases associated with different types of orbits in phase space: librational motion at low energy and rolling motion at high energy.

The rolling spool is analogous to a point particle moving in a U-shaped potential for which, once the energy E has been fixed, the orbit in phase space is uniquely determined; the system is *monocyclic* and it satisfies the requirement of ergodicity. [9] When its motion is librational, the spool moves back and forth between two turning points $x_{\pm}(E)$, and draws closed orbits in phase space with period $\tau(E)$. Figure 4 shows a contour plot of various energy levels in phase space for the rolling spool: (a) for energy $E = E_c$ we have a separatrix, (b) below E_c the curve of constant energy is a closed curve (an ellipse for very low energies), whereas for values of E larger than E_c it becomes an open curve. This corresponds to two different behaviours of the spool: (i) the spool oscillates around an equilibrium point (ii) the spool rolls along the plane. According to refs.[8] and [12] we can interpret the two cases as two distinct phases. We can define the *ordered phase,* corresponding to librational motion; and the *disordered phase*, corresponding to rolling motion.

Next we define a *parameter*, Θ_{AKE}, proportional to the kinetic energy averaged over one period, sometimes called *temperature in one-dimensional mechanical models of thermodynamics*[9,30].

$$\Theta_{AKE}(E) \equiv \frac{2}{k_B \tau(E)} \int_0^{\tau(E)} dt K\left[p(t;E)\right] = 2\frac{\langle K \rangle}{k_B} \tag{6}$$

Note, however, that in our case the parameter defined by eq.(6) is *not* the control parameter governing the phase transition: in the second order transition we are discussing, as will become clearer later, the control parameter is the total energy *E* of the system.
The kinetic energy of the spool averaged over one period can be computed numerically for different values of the total energy. In Figure 6(A) (dashed lines) we show the dependence of kinetic energy $\langle K \rangle$ on total energy, E. The plot highlights the presence of a critical point at $E = U_{\max}$ ($U_{\max} = E_c = 2M_W gr$). Eq.(6) allows us to compute Θ_{AKE}, and obtain the total energy E (Fig.6 (A)) as a continuous function of Θ_{AKE} with a discontinuous derivative C,

$$C = \left[\frac{\partial E}{\partial \Theta_{AKE}}\right] = \frac{k_B}{2}\left[\frac{\partial E}{\partial \langle K \rangle}\right]. \tag{7}$$

Fig.6 (C), where C is reported as a function of the total energy, shows that the values of *C* in the limits of low and high energies are k_B e $k_B/2$ respectively. These values can be compared with the heat capacity at constant volume for a monoatomic gas ($k_B/2$ per degree of freedom for each molecule), and for a solid in the classical approssimation (k_B per degree of freedom for each molecule) to conclude that the rolling spool mimics the behaviour of a monoatomic, one dimensional thermodynamic system and that the values of *C* distinguish the ordered phase from the disordered one.

In the following we will always consider the equation of motion for the spool for $\lambda \ll 1$, but not necessarily for small angles. This means that we will use the equation of motion

$\ddot{\vartheta} = -\frac{gM_W r}{I_0}\sin(\vartheta)$; and in order to compute the behavior of the system near the critical point, we will use large angle approximations.

With the aim of characterizing in detail the phase transition we introduce, according to ref.[12], the *order parameter* $\psi = \cos\left(\frac{\vartheta_A}{2}\right)$, where $\vartheta_A \in [-\pi, \pi]$ is the value of the angle ϑ at the time instant in which the kinetic energy of the rolling is minimum (if the spool is oscillating, it corresponds to the value of the angle at maximum amplitude). As required, the value of order parameter is nonzero in the ordered phase (oscillatory motion) while it vanishes in the disordered phase.

From eq.(3) we can derive an equation for the value of the order parameter:

$$U_{MAX} = U(\vartheta_A) = 2Mgr\sin^2(\frac{\vartheta_A}{2}) = E_c\left(1-\psi^2\right) \rightarrow \psi^2 = \frac{E_c - U_{MAX}}{E_c} \tag{8}$$

where $E_c = 2M_W rg$ is is the minimum energy allowing the transition from librational to rotational motion. Eq. (8) allows to find the values of ψ in the librational phase when $E \le E_c$; indeed in this case $U_{\max} = E$ and

$$\psi^2 = \frac{E_C - E}{E_C} \rightarrow \psi = \pm\sqrt{\frac{E_C - E}{E_C}} \tag{9}$$

This trend is typical of the order parameter in the Landau theory of second order phase transitions. For $E > E_c$, $E_c - U_{MAX} = 0$ and the only possible value for ψ is zero. The previous results can be compactly expressed by requiring that ψ minimizes the potential function

$$F(\psi, E) = \frac{E_C\psi^4}{2} + \left(E - E_C\right)\psi^2 + F_0 \tag{10}$$

Infact by setting $\frac{\partial F}{\partial \psi} = 0$ one finds

$$E_C\psi^3 + \left(E - E_C\right)\psi = 0 \tag{11}$$

And requiring the solutions to be minima, the extra value $\psi = 0$ for $E \le E_c$ is discarded. The experimental values of ψ as a function of the total energy, obtained measuring the maximum value of kinetic energy during the motion, are reported in Fig.6B. This behaviour is in agreement with the fact that at a second order phase transition, the order parameter increases continuously from zero, starting at the critical value of the critical parameter (here the total energy) of the phase transition.

We next discuss how the divergence of the period of the spool can be interpreted as a critical slowing of the relaxation time, i.e. the time needed for the order parameter to settle at a definite value. Assuming the spool is in the librational phase, we use eq.(5) for the small amplitude period $\tau_0 = 2\pi\sqrt{\frac{I_0(1-\lambda)}{M_W rg}}$ and use the Kidd-Fogg [31] approximation to the complete elliptic integral of the first kind, which gives

$$\tau \approx \frac{\tau_0}{\sqrt{\cos\left(\vartheta_A/2\right)}} = \frac{\tau_0}{\sqrt{\psi}} = \tau_0 \left(\frac{E_C}{E_C - E} \right)^{\frac{1}{4}} \tag{12}$$

.

A similar behaviour also can be seen beyond the critical point. In this case the spool undergoes rolling motion, and for energies little higher than the critical point ($E - E_C \ll E_C$) it can be proven [32] that the period of rotation is simply half the period of oscillation corresponding to the same value of $\left|E - E_C\right|$.

$$\tau \approx \frac{1}{2}\tau_0 \left(\frac{E_C}{E - E_C} \right)^{\frac{1}{4}} \tag{13}$$

So we see a critical slowing down (divergence of the relaxation time), which on both sides of the phase transition behaves like $\tau \sim \left|E - E_C\right|^{-\frac{1}{4}}$.

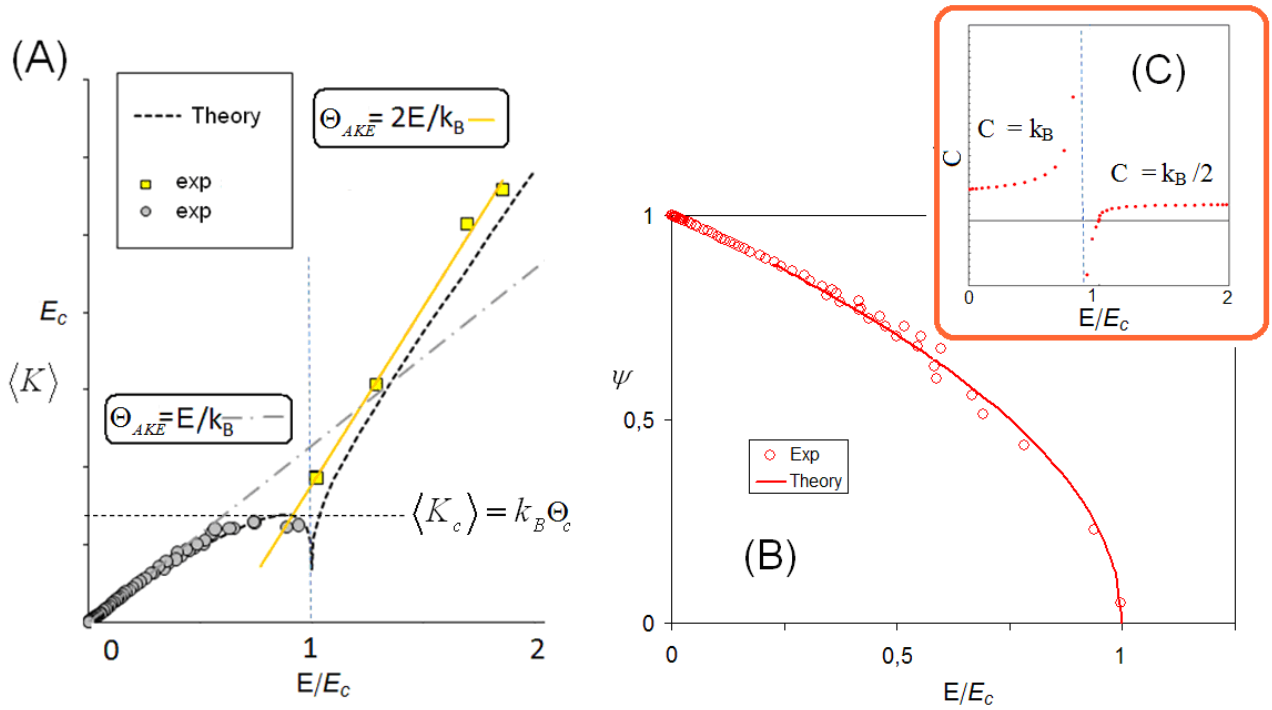

Figure 6 (A) Experimental measurements of kinetic energy as a function of the total energy. The relation between Θ_{AKE} and E computed numerically (dashed lines) shows the presence of a critical point. Dots and squares represent experimental values. The fitting parameters for the slopes at low ($m = 1.1 \pm 0.1$) and high energy ($m = 2.3 \pm 0.1$) confirm that the rolling spool behaves analogously to a monoatomic thermodynamic system undergoing a transition from a solid to a gaseous phase. The relation between $\langle K \rangle$ and E computed numerically (dashed lines) shows the presence of a critical point. Dots and squares represent experimental values. The parameter ψ (B measured) and the derivative C (C numerically calculated) are plotted as a function of the total energy, also highlighting the presence of a critical point . Note that the function $\langle K \rangle (E)$ is not strictly increasing; thus, below a critical value $\langle K_C \rangle$ different values of the total energy E (pertaining to both librational and rotational states) correspond to the same value of $\langle K \rangle$. At the critical value $\langle K_C \rangle$, according eq.(7), C diverges and changes sign.

Because of its remarkable properties, the asymmetric rolling spool can be discussed with students to focus on the mechanical principles underlying thermodynamics laws. In particular, the role of the Virial theorem can be highlighted. In fact, for small oscillations and energies the behaviour of the system is approximately harmonic. In this case, the time averages of kinetic and potential energy are the same; and the kinetic energy is approximately half the total energy (so $C = k_B$). However, as the energy of the system increases and becomes much higher than the threshold of rolling motion (a situation analogous to the gaseous state), the potential energy of the system becomes increasingly negligible, and kinetic energy becomes, asymptotically, equal to the total energy (leading to $C = k_B/2$).

In this line, more complex systems could be considered. In the appendix, for example, a similar behaviour is shown for a one-dimensional system of some practical relevance, an ensemble of a small number of inter-penetrable soft spheres with a reciprocal repulsive Gaussian core potential [33-36].

V. A MODEL OF SLIDING FRICTION

We show in this section how the rolling spool can help visualizing the Tomlinson model for sliding friction between solids [21].

The empirical laws for sliding friction forces, proposed by Amontons (1699) and Coulomb (1785), as the result of a series of careful investigations [37], are generally presented in physics textbooks [38] as:

(I) The direction of the static friction force acting on a body in contact with a surface is opposite to the direction of the net force which would accelerate the object with respect to the surface and its magnitude satisfies:

$$f_s \leq \mu_s N \tag{6}$$

where the dimensionless constant μ_s is called the coefficient of static friction and N is the magnitude of the normal force. The equality sign in eq. (6) holds only at the threshold of motion.

(II) The direction of the kinetic friction force acting on an object is opposite to the direction of the object's sliding motion relative to the surface and its magnitude is given by

$$f_k = \mu_k N \tag{7}$$

where μ_k is the coefficient of kinetic friction[3].

The values of μ_k and μ_s depend on the nature of the surfaces, but μ_k is generally less than μ_s.

As a consequence of (6) and (7) the acceleration as function of the applied force has a discontinuity. In Fig. 7 (A) we show the relationship between the external force, F_{ext}, acting on the block and its acceleration. The presence of a sharp discontinuity near a threshold value of the force signals a critical phenomenon with the characteristics of a phase transition, which should be clarified at the microscopic level.

For this purpose, we consider the Tomlinson model, also known as the Prandtl-Tomlinson Model [22], widely used as the basis for many investigations on frictional mechanisms at the mesoscopic scale. Prandtl considered the one dimensional motion of a particle in a periodic potential $U_{PT}(x) = \mu \frac{N}{k}\cos(kx)$, subject to an external force F and to a viscous-type force term:

$$m\ddot{x} = F - \eta\dot{x} - \mu N \sin(kx) \tag{8}$$

Here, x is the coordinate of the particle m its mass, F the external force acting upon it, η the damping coefficient, μN the amplitude of the periodic force, and k its "wave number".

According to the Tomlinson model, if a body is at rest and a force F is applied to it, then its equilibrium position moves to the point x, which satisfies the equation $F_{\text{ext}} = \mu \text{N} \sin(kx)$. This equation has a solution only when $F_{\text{ext}} \leq \mu \text{N}$. So, the threshold force of static friction, in this model, is equal to $F_{\text{s}} = \mu N$. For a larger force, no equilibrium is possible and the body initiates macroscopic motion.

The rolling spool mimics the dynamics of a particle in the potential $U_{PT}(x)$ with the identifications $m \equiv \langle M_{eff} \rangle$, $k \equiv 2\pi/R$, $\eta = 0$ and $\frac{\mu N}{k} \equiv M_W g r$; and provides an intuitive representation of the discontinuity appearing in Fig.7 (A and B) at the critical force to get the motion started.

[3] A more precise formal defininition of the friction force which takes into account the dependence on the direction of the relative velocity is given, for example, in ref. [44] eq.(2) $f_k = -\mu_k N \cdot \text{sign}(v_{rel})$

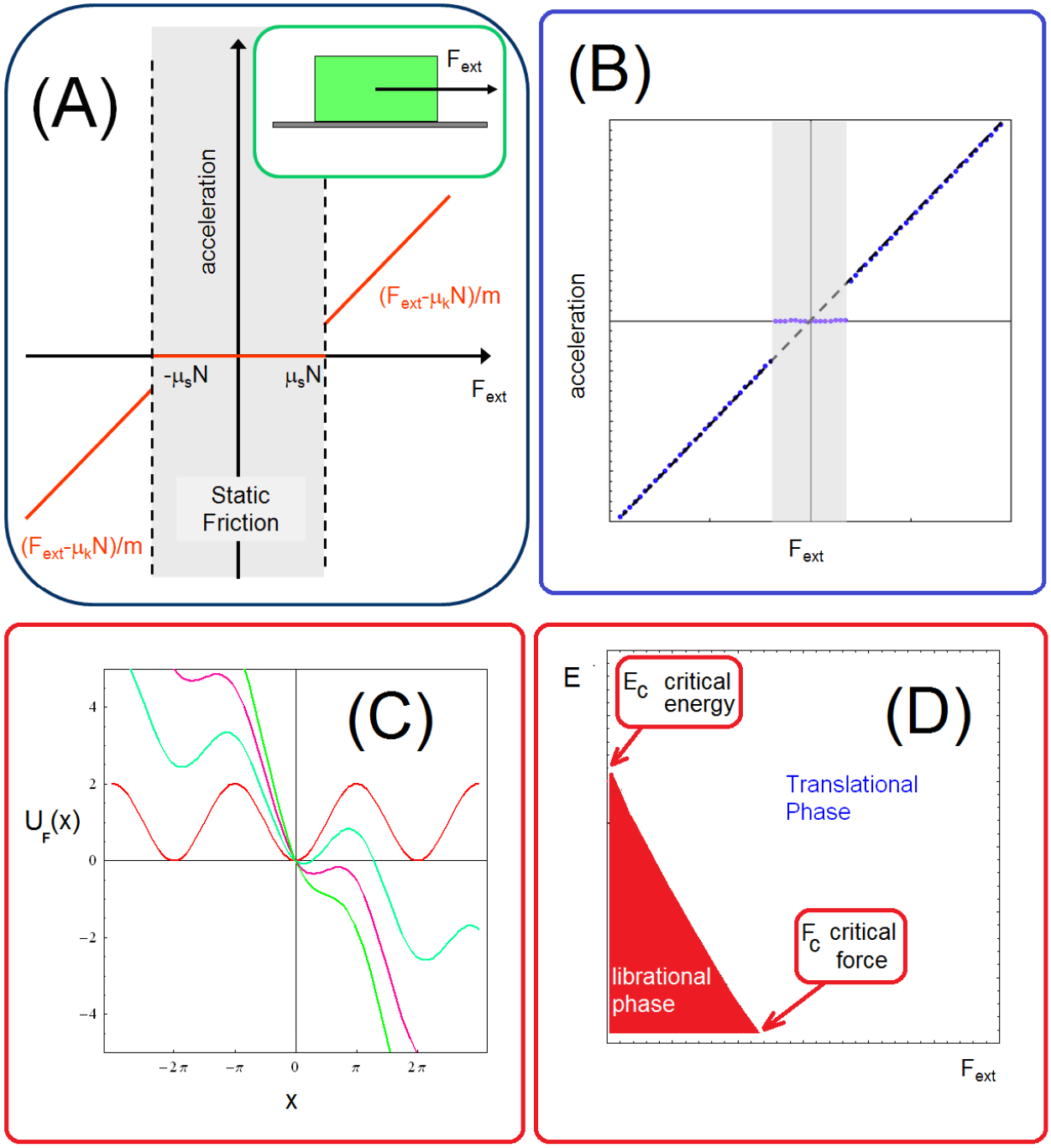

Figure 7 (A) Macroscopic law of friction dependence of the acceleration on the external force according to the Coulomb theory. (B) Dependence of the average acceleration on the external force when $\eta = 0$, i.e. without kinetic friction as for the rolling spool. (C) Potential of the asymmetric rolling spool for several values of the external driving force. (D) Phase diagram showing the translational and librational regimes of the spool in the external force - gravitational potential energy plane.

Using the same approach as in section III.C, we can characterize the passage of the system from static to kinetic sliding friction condition as a phase transition driven by the external force.
We introduce the potential obtained by taking into account the external force:

$$U_F(x) = M_W gr(1 - \cos(x/R)) - F_{ext} x \,.$$

When the external force vanishes, $U_F(x)$ is a symmetric potential with symmetric degenerate minima. The critical energy, E_c, to have a phase transition from librational to rolling motion, i.e. the

energy needed to escape from the potential well, is given by $E_c = Max(U_F(x)) = 2M_W gr$. The presence of a non vanishing force causes a symmetry breaking in the potential $U_F(x)$ which now has the first local minimum between $x = 0$ and $x = \pi$ while if $F_{ext} > F_c$ no minima are allowed (F_c . can be calculated for E=0 as $F_c \approx 0.38\frac{2M_W gr}{R}$). Thus the librational phase is forbidden for $F_{ext} > F_c$ and in general for strong force and high energy. The distinct translational and librational regimes for the motion of the asymmetric rolling spool can be conveniently represented on a plane whose axes correspond to the external force F_{ext} and the energy E (Fig.7.D).

DISCUSSION AND CONCLUSIONS

In this paper we presented some simple experiments aimed to explore quantitatively the physics of rotation and oscillations of an asymmetric rolling spool. Measurements were made using the Tracker Video Analysis software.
A detailed comparison between theoretical expectations and experimental results was discussed.
The rolling spool with an extra mass at low energies, and with a low degree of azimuthal asymmetry, behaves like a simple pendulum. Analogously to the pendulum, the motion of the unbalanced spool is due to the gravitational force and to the geometry of the constraints, i.e. to the competitive action of the gravitational force and the sliding friction force. The period of the oscillations depends on the amplitude and diverges when the amplitude approaches a critical value above which the system undergoes a rotational non periodic motion.
This critical behaviour suggests the presence of a phase transition, analysed by defining appropriate thermodynamic variables for the mechanical system. In this way, the rolling spool mimics the gas/solid transition in a mono-atomic thermodynamic system.
This phase transition can be used to describe the critical switch from static to dynamic sliding friction near the threshold since the rolling spool models the behaviour of a particle moving in the Tomlinson potential.
The experiments can be realized and analysed using only inexpensive materials and open source tools. The phenomena highlighted deal with relevant topics in the physics curriculum, and appear appropriate to be used in high school and undergraduate physics courses. The theoretical approach clarifies important connections between mechanics and thermodynamics and could have significant educational implications.

APPENDIX

Consider a system of inter-penetrable soft spheres confined to a one dimensional box. By this expression we mean a collection of particles interacting with each other through a soft repulsive potential of finite height, and constrained to move on a line segment with reflecting endpoints. In particular we use a Gaussian core repulsive potential [33-36]
A similar arrangement (often in more than one dimension) has been used to model the behaviour of polymers and colloids. Initially the particles are placed at equal distances in the box, so that each one is in a minimum for the potential created by its two nearest neighbours. Furthermore the parameter is chosen so that the equilibrium effective potential felt by each particle best approximates a harmonic potential (i.e. particles are initially placed near a zero of the third derivative of the potential). The initial disposition is depicted in figure 8.

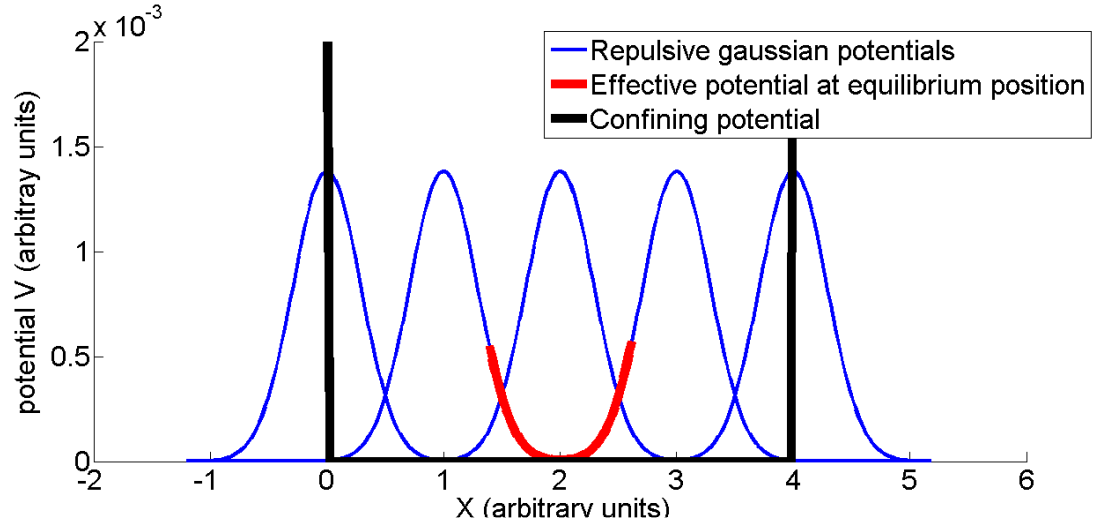

Figure 8 : Initial arrangements of inter-penetrable particles with Gaussian core potential.

Simulations are run for increasing values of the initial kinetic energy of the particles, and the time averages of kinetic energy K and total energy E are computed. Results are reported in figure 9.

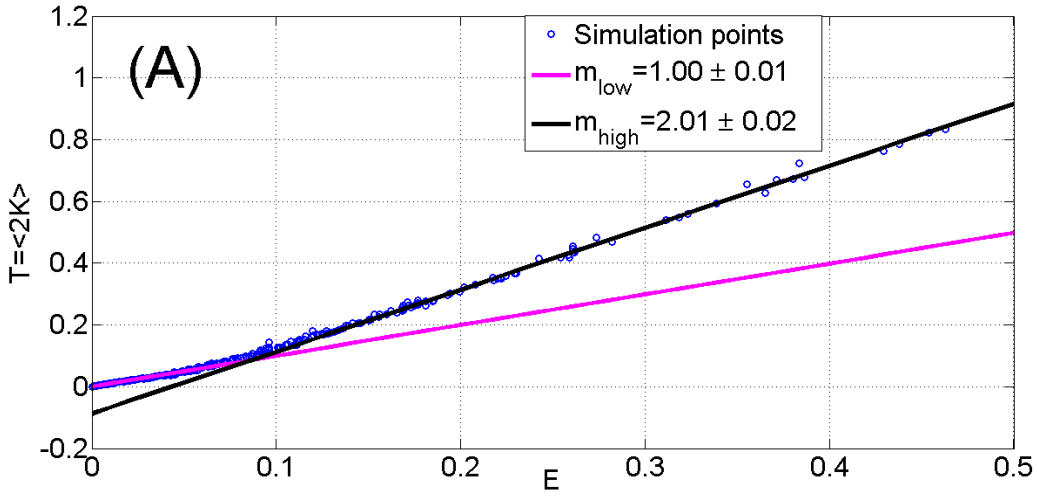

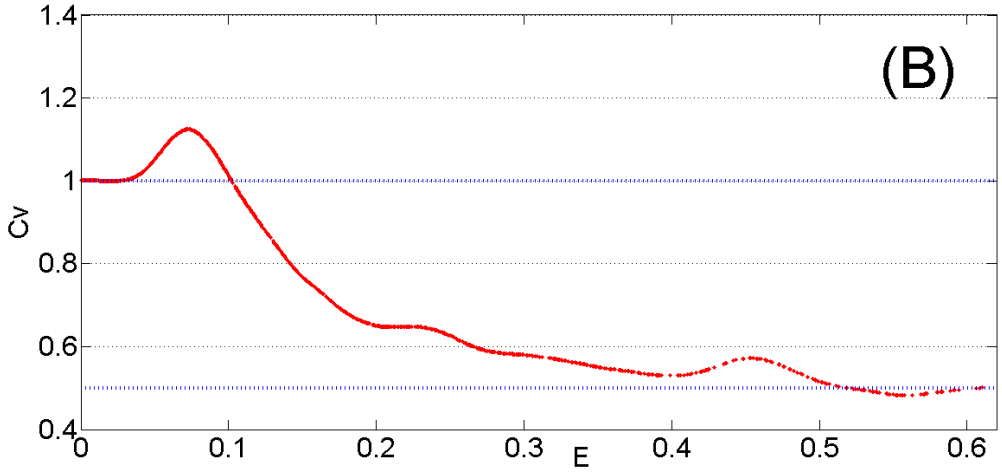

Figure 9: "Solid-gas" phase transition in an inter-penetrable soft sphere system with repulsive Gaussian-core potential. (A) Relationship between temperature and total energy. (B) heat capacity.

At low energies, particles oscillate around their equilibrium position and, since the effective potential is approximately harmonic, the time averages of kinetic and potential energies are equal. At high energies, particles can interpenetrate each other, and their behaviour asymptotically approaches that of a non interacting particle (ideal) one dimensional gas.

BIBLIOGRAPHY

[1] Sivardiere J 1997 Simple mechanical models exhibiting instabilities *Eur. J. Phys.* **18** 384
[2] Charru F 1997 A simple mechanical mimicking phase transition *Eur. J. Phys.* **18** 417
[3] Sharpe J P and Sungar N 2010 Supercritical bifurcation in a simple mechanical system: an undergraduate experiment *Am. J. Phys.* **78** 520
[4] Bobnar J, Susman K, Parsegian V, Rand P, Čepič M, Podgornik R 2011 Euler strut: a mechanical analogy for dynamics in the vicinity of a critical point *Eur. J. Phys.* **32** 1007-1018
[5]Drumheller J E, Raffaelle D and Baldwin M 1986 *Am. J. Phys.* **54** 1130–3
[6] Fletcher G 1997 A mechanical analog of first- and second-order phase transitions *Am. J. Phys.* **65**, 74-81
[7] Ochoa F and Clavijo J 2006 Bead, hoop and spring as a classical spontaneous symmetry breaking problem *Eur. J. Phys.* **27** 1277
[8] Baeten M and Naudts J 2011 On the Thermodynamics of Classical Micro-Canonical Systems *Entropy* **13** 1186-1199
[9] Campisi M and Kobe D H 2010 Derivation of the Boltzmann principle *Am. J. Phys* **78** 608-615
[10] Gallavotti G. 1995 *Statistical mechanics. A short treatise* (Berlin: Springer Verlag)
[11] S. Hilbert and J. Dunkel 2006 Nonanalytic microscopic phase transitions and temperature oscillations in the microcanonical ensemble: An exactly solvable 1d-model for evaporation *Phys. Rev. E* **74**, 011120
[12] Onorato P, Malgieri M, DeAmbrosis 2014 Phase transitions in one dimensional mechanical models of thermodynamics and the physics of the Hall bar system *Physics Letters A* **378** 590-596
[13] Jensen J H 2011 Rules for rolling as a rotation about the instantaneous point of contact *Eur. J. Phys.* **32** 389–97
[14] B Y-K Hu 2011 Rolling of asymmetric discs on an inclined plane *Eur. J. Phys*. **32** L51–44.
[15] Holm D D 2008*Geometric Mechanics Part II: Rotating, Translating and Rolling* (London: Imperial College Press).
[16] Besson U, Borghi L, De Ambrosis A, Mascheretti P 2010 A ThreeDimensional Approach and Open Source Structure for the Design and Experimentation of TeachingLearning Sequences: The case of friction *International Journal of Science Education* **32** 1289-1313.
[17] Fletcher 2002 N H Harmonic? Anharmonic? Inharmonic? *Am. J. Phys.* **70** 12
[18] Thomchick J and McKelvey J P 1978 Anharmonic vibrations of an 'ideal' Hooke's law oscillator, *Am. J. Phys*. **46**, 40–45
[19] Pecori B Torzo G, and Sconza A 1999 Harmonic and anharmonic oscillations investigated by using a microcomputer-based Atwood's machine *Am. J. Phys*. **67**, 228–235
[20] Mohazzabi P 2004 Theory and examples of intrinsically nonlinear oscillators *Am. J. Phys.* **72**, 492–498
[21] Tomlinson G A 1929 A molecular theory of friction, *Philos. Mag.* **7**, 905–939
[22] Prandtl L 1928 Ein Gedankenmodell zur kinetischen Theorie der festen Korper, *Journal of Applied Mathematics and Mechanics/Zeitschrift für Angewandte Mathematik und Mechanik* **8** 85-106
[23] Popov V L 2010 *Contact Mechanics and Friction* (Berlin Heidelberg: Springer-Verlag)

[24] http://www.compadre.org/osp/webdocs/tools.cfm?t=Tracker
[25] Phommarach S, Wattanakasiwich P and Johnston I 2012 Video analysis of rolling cylinders *Phys. Educ.* **47** 189
[26] Heck A and Uylings P 2010 In a hurry to work with high-speed video at school? *Phys. Teach.* **48** 176–81; Vollmer M and Mollmann K 2011 High speed and slow motion: the technology of modern high speed cameras *Phys. Educ.* **46** 191–202; Brown D and Cox A J 2009 Innovative uses of video analysis *Phys. Teach.* **47** 145–50
[27] Gomez R W, Hernandez-Gomez J J and Marquina V A 2012 Jumping cylinder on an inclined plane *Eur. J. Phys.* 33 1359–1365
[28] Turner L and Turner A M 2010 Asymmetric rolling bodies and the phantom torque *Am. J. Phys.* **78** 905
[29] Malgieri M, Onorato P, Mascheretti P, De Ambrosis A 2013 Reconstruction of a "gedanken" Huygens' experiment and measurements based on video analysis tools *Eur. J. Phys.* **34** 1145–1157
[30] Cardin, F., and M. Favretti. 2004 On the Helmholtz-Boltzmann thermodynamics of mechanical systems. *Continuum Mechanics and Thermodynamics* 16.1-2: 15-29.
[31] Kidd, R. B., & Fogg, S. L. 2002. A simple formula for the large-angle pendulum period. *The Physics Teacher*, 40(2), 81-83.
[32] Butikov, E. I. 1999. The rigid pendulum-an antique but evergreen physical model. *European Journal of Physics*, 20(6), 429.
[33] Stillinger F H 1976 Phase transitions in the Gaussian core system *The Journal of Chemical Physics* **65** 3968.
[34] Stillinger F H and Weber T A 1978 Study of melting and freezing in the Gaussian core model by molecular dynamics simulation *The Journal of Chemical Physics* **68** 3837.
[35] Mausbach P, Ahmed A and Sadus R J 2009 Solid-liquid phase equilibria of the Gaussian core model fluid *The Journal of Chemical Physics* **131**, 184507
[36] Prestipino S, Saija F and Giaquinta P V 2005 Phase diagram of the Gaussian-core model *Phys. Rev. E*, **71**, 050102
[37]. Coulomb, C A 1785 Théories des machines simples [Theory of simple machines] *Mém. Math. Phys. Acad. R. Sci.* **10***,* 161–342. (Reprinted by Bachelier, Paris, 1821)
[38] Halliday D, Resnick R, Walker J 2007 *Fundamentals of Physics Extended 8th edition* (New York: John Wiley & Sons)